Biliary cholesterol crystallization characterized by single-crystal cryogenic electron diffraction

Daphne Weihs,[1],* Judith Schmidt,* Ilana Goldiner,[†] Dganit Danino,[2],* Moshe Rubin,[§] Yeshayahu Talmon,[3],* and Fred M. Konikoff[†]

Department of Chemical Engineering,* Technion–Israel Institute of Technology, Haifa 32000, Israel; Department of Gastroenterology,[†] Tel Aviv Sourasky Medical Center and Minerva Center for Cholesterol Gallstones and Lipid Metabolism in the Liver, Sackler Faculty of Medicine, Tel Aviv University, Tel Aviv 69978, Israel; and Department of Surgery,[§] and Felsenstein Research Center, Rabin Medical Center, Petah-Tikva 49100, Israel

Abstract Cholesterol crystals are the building blocks of cholesterol gallstones. The exact structure of early-forming crystals is still controversial. We combined cryogenic-temperature transmission electron microscopy with cryogenic-temperature electron diffraction to sequentially study crystal development and structure in nucleating model and native gallbladder biles. The growth and long-term stability of classic cholesterol monohydrate (ChM) crystals in native and model biles was determined. In solutions of model bile with low phospholipid-to-cholesterol ratio, electron diffraction provided direct proof of a novel transient polymorph that had an elongated habit and unit cell parameters differing from those of classic triclinic ChM. This crystal is exactly the monoclinic ChM phase described by Solomonov and co-workers (*Biophysical J.*, In press) in cholesterol monolayers compressed on the air–water interface. We observed no evidence of anhydrous cholesterol crystallization in any of the biles studied.⬛ In conclusion, classic ChM is the predominant and stable form in native and model biles. However, under certain (low phospholipid) conditions, transient intermediate polymorphs may form. These findings, documenting single-crystal analysis in bulk solution, provide an experimental approach to investigating factors influencing biliary cholesterol crystal nucleation and growth as well as other processes of nucleation and crystallization in liquid systems.—Weihs, D., J. Schmidt, I. Goldiner, D. Danino, M. Rubin, Y. Talmon, and F. M. Konikoff. Biliary cholesterol crystallization characterized by single-crystal cryogenic electron diffraction. *J. Lipid Res.* 2005. **46:** 942–948.

Supplementary key words   bile • gallstones • cholesterol monohydrate • anhydrous cholesterol

Excess body cholesterol is excreted from the liver via bile either after conversion to bile salts or as free cholesterol. Although bile salts are readily water soluble, cholesterol is not. Therefore, the hydrophobic cholesterol molecules are solubilized in bile within mixed-lipid aggregates (micelles and vesicles) composed mainly of bile salts and phospholipids. When the solubilization capacity of these aggregates is exceeded, cholesterol starts to precipitate, and a process leading to gallstone formation begins (1). The physical configuration and transformation of the biliary lipid microstructures involved in cholesterol gallstone formation are still incompletely understood. In particular, little is known about the initial steps of cholesterol crystal nucleation and growth.

Cholesterol monohydrate (ChM) crystals, the end product of biliary cholesterol precipitation in aqueous solutions, have a triclinic crystal structure and a rhomboid, plate-like macroscopic shape (2, 3). In lithogenic biles, these plate-like crystals can be easily identified by polarized light microscopy on the basis of their characteristic morphology and birefringence properties (4). ChM crystals have been identified by electron microscopy (5, 6) and X-ray diffraction techniques (7). It had been suggested that cholesterol gallstones also contain anhydrous cholesterol (8), but this has been disputed as a drying artifact of sample preparation (9). A variety of cholesterol crystal habits were later observed in nucleating model and native biles (10, 11). Some of those crystals had mass density and morphological characteristics that suggested anhydrous cholesterol crystallization (12). Furthermore, X-ray

Abbreviations: ChIn, cholesterol intermediate; ChM, cholesterol monohydrate; cryo-ED, cryogenic temperature electron diffraction; cryo-TEM, cryogenic temperature transmission electron microscopy; CSI, cholesterol saturation index; TLC, total lipid concentration.

[1] Present address of D. Weihs: Departments of Pathology and Chemistry, David Geffen School of Medicine, UCLA, Los Angeles, CA 90095.

[2] Present address of D. Danino: Department of Biotechnology and Food Engineering, Technion–Israel Institute of Technology, Haifa 32000, Israel.

[3] To whom correspondence should be addressed.
   e-mail: ishi@tx.technion.ac.il

diffraction data have supported the suggestion that biliary cholesterol crystallization may involve initial anhydrous crystallization (10). However, early crystals could not be reliably distinguished from mature ChM crystals by the methods used to date.

In this study, we employed single-crystal cryogenic-temperature electron diffraction (cryo-ED) to study biliary cholesterol crystallization. Electron diffraction was combined with cryogenic-temperature transmission electron microscopy (cryo-TEM) and digital light microscopy to directly visualize the crystals and other microstructures present in nucleating bile solutions (13–15). Electron diffraction is an analytical technique that provides information on unit cell parameters of micrometer-scale crystals within solution. For the first time, diffraction data from single cholesterol crystals have been obtained in bulk solutions of nucleating bile in its fully preserved native state.

MATERIALS AND METHODS

Materials

Egg yolk phosphatidylcholine, 99% pure, (Avanti Polar Lipids, Inc.; Alabaster, AL) was used as obtained. Cholesterol and sodium taurocholate, >98% pure, (Sigma Chemical Co.; St. Louis, MO) were used after recrystallization. All other chemicals and solvents were American Chemical Society (ACS) reagent grade and were used without further purification. Glassware was acid washed and thoroughly rinsed in distilled water.

Model bile

Model biles were prepared from a mixture of cholesterol (in chloroform), egg yolk phosphatidylcholine (in chloroform), and sodium taurocholate (in methanol), at predetermined molar ratios (see below). After drying under N_2, the mixture was dissolved in chloroform-methanol (2:1; v/v) and dried again under N_2 at reduced pressure for 18 h and kept at $-4°C$. The dried lipid film was resuspended in saline (150 mM NaCl, 3 mM NaN_3, pH 6–7) to the required final total lipid concentration (TLC). The solution was incubated at 56°C for 1 h, resulting in a clear, isotropic solution free of large particles, as determined by light microscopy. To start the cholesterol crystallization process (10), solutions were cooled to 37°C. This time point was defined as "time zero."

Two previously well-characterized model bile solutions were studied. The first (Model A) has a lipid composition simulating that of lithogenic gallbladder biles of cholesterol gallstone patients (16) [lipid composition: 18.4 mM cholesterol, 36.9 mM egg yolk phosphatidylcholine, and 120 mM sodium taurocholate; TLC, 10 g/dl; and a cholesterol saturation index (CSI) (17) of 147%]. The other model system (Model B) is a dilute, bile salt–rich model (0.36 mM cholesterol, 0.18 mM egg yolk phosphatidylcholine, 21.2 mM sodium taurocholate; TLC, 1.2 g/dl; CSI, 208%), which yields abundant non-plate-like cholesterol crystals in the nucleation process (10).

Native bile

Human gallbladder bile samples from cholesterol gallstone patients were obtained by cholecystectomy. Informed consent was obtained according to a protocol approved by the local institutional human subjects committee. Bile was aspirated by puncture of the gallbladder under laparoscopic assistance prior to manipulation of the gallbladder. The bile was centrifuged (Mi-crofuge, 5,000 g, 10 min, 25°C) to remove cell debris, 3 mM NaN_3 was added to avoid microbial contamination, and then samples were incubated under N_2 at 37°C. Biliary lipids were extracted by chloroform-methanol (2:1; v/v) and quantified as previously described: bile salt (18) and cholesterol (19) concentrations were determined enzymatically, and phospholipids were determined as described by Bartlett (20). The CSI was calculated using the critical tables of Carey (17). The compositions and characteristics of these biles are shown in **Table 1**.

Standard cholesterol crystals

Standard monohydrate and anhydrous cholesterol crystals, which served as controls for electron diffraction studies, were prepared as previously reported (3). Both types of crystals were precipitated from solution directly onto a carbon-coated, 200-mesh microscopy grid at room temperature and then cooled in liquid nitrogen to enhance crystal stability under the electron beam. ChM crystals were precipitated from a solution of cholesterol in 99.8% absolute ethanol (Frutarom; Haifa, Israel), whereas anhydrous crystals were precipitated from a solution of cholesterol in 99.7% glacial acetic acid (Frutarom).

Digital light microscopy

Bile samples ($\sim$200 μl) were placed on a glass slide (Clay-Adams) and observed at 25°C using an Olympus BH-2 light microscope. Images were obtained in the differential interference contrast (Nomarski optics) and the crossed polarizers modes. Images from the light microscope were directly recorded by an Optronics 750 LE-D digital camera (Optronics; Goleta, CA) connected to a personal computer. Image processing was performed with the Adobe Photoshop 5.0 software package (Adobe Systems, Inc.; San Jose, CA).

Cryo-TEM and cryo-ED

Native and model samples were obtained sequentially, vitrified at different time points to follow the crystal growth process. Vitrified specimens of native and model bile were prepared for transmission electron microscopy (TEM) in a controlled environment vitrification system at 37°C and 100% relative humidity, as previously described (21). In brief, a drop was applied onto a perforated carbon film, supported on an electron microscopy copper grid, and held by tweezers in the vitrification system chamber. The sample was blotted for thickness and immediately plunged into liquid ethane at its freezing point ($-183°C$). The vitrification process captures microstructures and crystals in the sample in a state as close as possible to the native state without the need for artifact-inducing staining or drying methods (22). Structures larger than $\sim$300 nm in diameter are blotted off or may be distorted or positioned flat within the liquid film. Thus, large crystals are always found flat on the grid. Standard crystals (see above) that served as controls were prepared at room temperature and then cooled to liquid nitrogen temperature for sample stability. An Oxford CT3500 cooling-holder (Gatan; Pleasanton, CA) was used to load the specimens into the TEM. Images and electron diffraction patterns were recorded in the low-dose mode to minimize electron beam radiation damage to the very radia-

TABLE 1. Lipid composition and cholesterol saturation of human biles

No.	Cholesterol	Phospholipids	Bile Salts	TLC	CSI
	mM	*mM*	*mM*	*g/dl*	*%*
1	14.2	30.7	91.7	7.9	147
2	3.8	7.2	23.0	1.9	214
3	5.6	16.0	59.2	4.6	118

TLC, total lipid concentration; CSI, cholesterol saturation index.

tion-sensitive samples. A Gatan MultiScan791 cooled CCD camera operated with the Digital Micrograph 3.1 software package (Gatan), was used to acquire the images and diffraction patterns. Images were recorded at nominal underfocus of 2–4 μm to enhance phase contrast. Selected-area electron diffraction patterns were obtained from several crystals identified by imaging at low and medium magnifications of 3,400× and 40,000×, respectively.

RESULTS

The crystallization processes of two model biles and three native biles were followed and documented. Model A had a lipid composition simulating that of lithogenic gallbladder biles. Model B, a dilute, bile salt–rich model, was previously shown to yield abundant non-plate-like cholesterol crystals in the nucleation process (10). In Model A, the crystallization process was preceded by the appearance of granular aggregates (as seen by Nomarski optics light microscopy) that were composed, as previously observed by cryo-TEM (15, 23), of spheroidal micelles, discoidal membrane patches, and unilamellar and multilamellar vesicles. Typical structures, observed by light microscopy in Model A and native bile, are presented in **Fig. 1**. Note in those images the coexistence, even after several days of incubation, of several different crystal morphologies. Classic rhomboidal crystals, with or without typical notch, (1 in Fig. 1) are observed alongside long and narrow crystals (2 in Fig. 1) as well as other crystal structures.

The earliest crystals observed by cryo-TEM were thin, long, and narrow, unlike the typical rhombus-shaped, mature ChM crystals visualized in the past at later stages by light microscopy (3, 14). **Figure 2A** shows crystals observed in vitrified specimens of Model A, 30 h after time zero. Note the typical notched structural feature of the cholesterol crystal (3) (arrow in Fig. 2A). The perforated carbon support film is seen in the background at low magnification. Figure 2B shows the corresponding electron diffraction pattern from the same crystal. The dark regu-
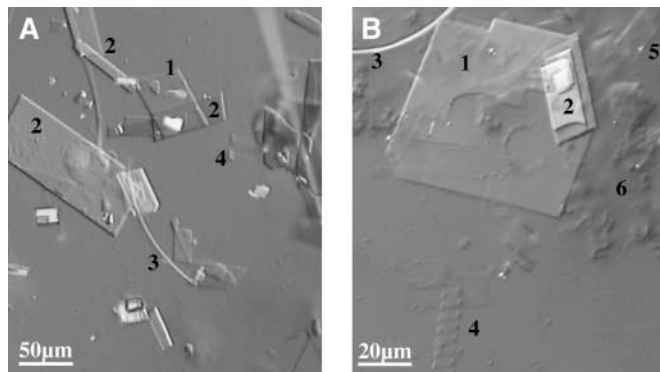

Fig. 2. Images and diffraction patterns of cholesterol monohydrate (ChM) crystals. A: Cryogenic temperature transmission electron microscope (cryo-TEM) image of a crystal in Model A, after 30 h. The arrowheads mark the edges of the crystal and the arrow marks the typical morphological notch in the crystal. The network structure in the background is the perforated carbon support film. B: Cryogenic temperature electron diffraction (cryo-ED) of the same Model A crystal. C: Cryo-TEM image of a crystal in native human bile no. 2, 3 days after removal from the patient. The arrowheads mark the edges of the crystal, and the beam stop indicates the region of diffraction. D: Cryo-ED of the native crystal in (C). E: Cryo-TEM image of a standard ChM crystal. The beam stop indicates the region of diffraction. F: Cryo-ED of the standard ChM crystal.

Fig. 1. Digital light microscopy in the Nomarski optics mode of model and native bile. A: Rhomboidal crystal (1), long and narrow crystals (2), arc (3), and helix (4) visualized in Model A after 16 days. B: Rhomboidal crystal with typical morphological notch in crystal (1), long and narrow crystals (2), arc (3), helix (4), tube (5) and aggregate clusters (6) observed in native human bile no. 2, 14 days after surgery.
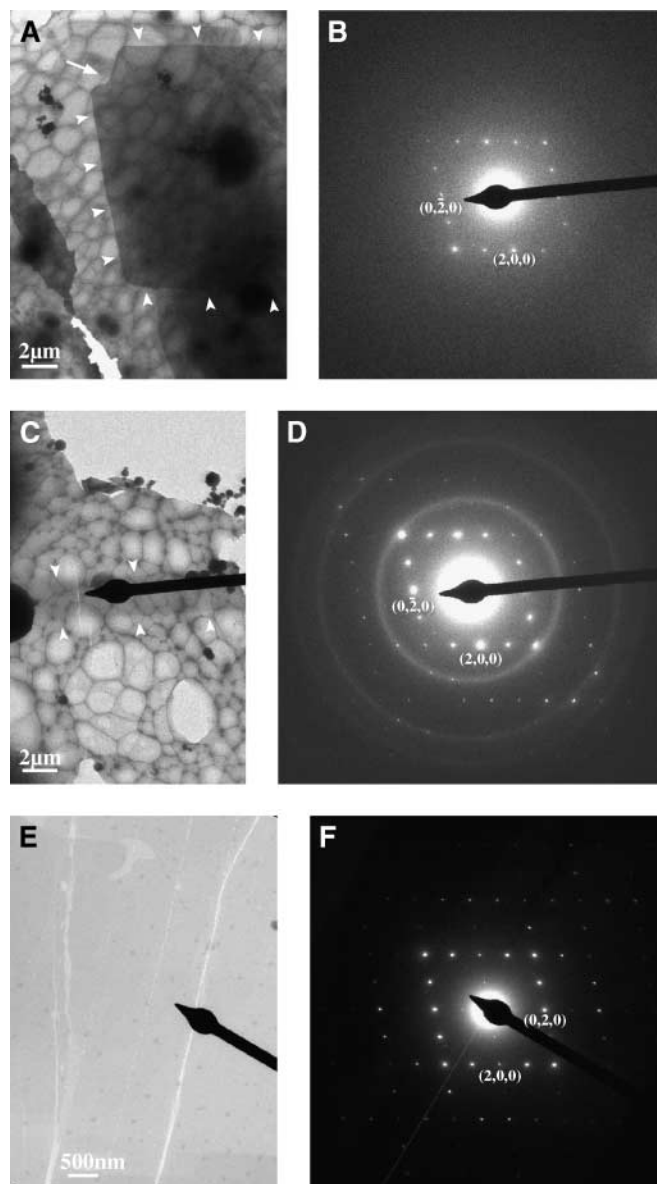
lar structure in the image is the beam stop, inserted to protect the detector from the intensity of the main undiffracted beam. The diffraction pattern in Fig. 2B shows a series of diffraction spots in a rhomboidal shape symmetrically surrounding the main undiffracted beam, which represent classic ChM crystals with a preferred zone axis of [001] relative to the electron beam.

Three native bile samples were studied by cryo-ED. The compositions and characteristics of these biles are shown in Table 1. Several crystals were observed, and all exhibited identical diffraction patterns. Thus, a single representative image is shown. The crystal habits were long, rectangular or classical, plate-like rhombus-shaped. Figure 2C shows a representative cryo-TEM image of a crystal seen in gallbladder bile number 2 (Table 1), 3 days after removal from the patient, and Fig. 2D is the corresponding cryo-ED pattern. This crystal had most likely begun to nucleate in the bile some time after time zero, because upon aspiration, samples are centrifuged and any existing crystals removed. The diffraction patterns of Fig. 2B, D exhibit identical d-spacings and angles between reflections. The d-spacing values of the diffraction patterns (two characteristic spots are marked on the image) agree with standard values to within 3% error, which can be attributed to measurement errors. The diffuse rings seen in Fig. 2D are produced by disordered crystalline ice together with vitreous ice. The brightest ring closest to the center corresponds to 3.7 Å. Both diffraction patterns are also identical to the diffraction pattern we obtained from a thin, standard ChM crystalline film, used as a reference, deposited on a carbon support film. Figure 2E is an electron micrograph of such a crystal, and Fig. 2F shows the corresponding diffraction pattern. The data of the latter two were recorded from a dry specimen, cooled to $-180°C$ to minimize electron beam radiation damage to the sensitive ChM crystals (see sample preparation).

In Model B, light microscopy showed initially only occasional few spheroidal aggregates. Filamentous crystal structures appeared after ~3 h, and were followed by arcs, helices, tubes, and helical tubes in a sequence, as reported previously (10). Eventually, an abundance of long, rectangular and classical, plate-like rhombus-shaped crystals were the dominating microstructures.

Electron microscopy revealed spheroidal micelles (3–5 nm in diameter) and unilamellar vesicles in two populations, of ~30 nm and 200–300 nm in diameter, particularly prior to the formation of crystals. Two types of transient, elongated crystals were identified by electron microscopy and diffraction. Both were from hundreds of nanometers to several micrometers long, and usually appeared multilayered or filamentous. The first type of crystal (**Fig. 3A**) was initially observed ~3 h after time zero, gradually became less abundant, and eventually disappeared altogether in a matter of ~6 h. The corresponding diffraction pattern for those crystals is shown in Fig. 3B. Note reflections $d_{2,0,2}$ (4.9 Å) and $d_{1,1,1}$ (5.8 Å), the two reflections that had been recorded earlier by powder X-ray diffraction (10), and had been attributed to anhydrous and monohydrate cholesterol. In cryo-electron diffraction, we are limited in our ability to tilt the sample. Therefore, we cannot reconstruct the crystal unit cell completely. We indexed these diffraction patterns according to information obtained by Solomonov et al. (24), who, in an independent study, obtained similar crystal structures. The second type of crystal (Fig. 3C, D; image and diffraction pattern, respectively) appeared at about the same time
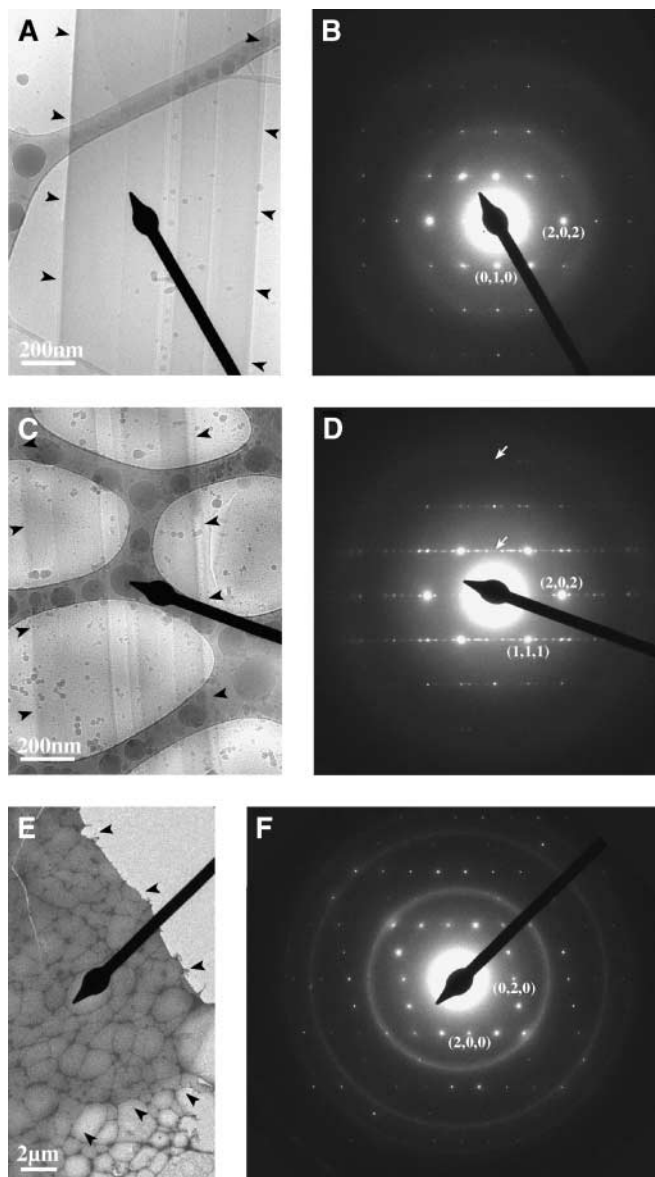

Fig. 3. Crystals in Model B. A: Cryo-TEM image of early-appearing, ribbon-like, transient crystals, 3 h after time zero. The arrowheads mark the edges of the crystal. The lacey structure in the background is the support film, and the dark specks are frost particles. B: Cryo-ED pattern of the early transient crystal. C: Cryo-TEM image of late-appearing transient crystals, 6 h after time zero. The arrowheads mark the edges of the crystal. D: Cryo-ED pattern of the crystal in (C). The arrows mark missing diffraction spots relative to the early polymorph. Note satellite spots appearing in this diffraction pattern. E: Cryo-TEM image of a ChM crystal. The arrowheads mark the edges of the crystal. F: Cryo-ED pattern of the same ChM crystal.

(~3 h) and was observed in vitrified specimens for several days after time zero. The diffraction pattern of the later-appearing transient consistently lacked some reflections obtained in the early phase, but was otherwise matching. Those differences may indicate that a process of change in structure was taking place. Most of the diffraction patterns of the longer-lasting crystal exhibited satellite points surrounding the main spots and on the same "horizontal" line. Several of the later-appearing transient crystals were of

a twisted ribbon structure, whereas others were slender and flat. Diffraction patterns of the twisted ribbons usually showed only the main reflections, without the satellite reflections seen in Fig. 3D, but were consistent with the longer-lasting transient crystals. ChM crystals of various plate-like habits appeared coexisting with the transient crystals from ~6 h and later (Fig. 3E). The diffraction pattern of the plate-like crystals (Fig. 3F) was identical to that of the standard ChM shown in Fig. 2.

Because earlier studies (10, 12) suggested the presence of anhydrous cholesterol in Model B, we collected, as reference, electron images and diffraction patterns of cooled (at −180°C), dry, thin films of anhydrous cholesterol deposited on carbon films from glacial acetic acid. A sample image and the corresponding diffraction pattern are shown in **Fig. 4**. Although the symmetry of the diffraction pattern is indistinguishable from that of the early intermediate crystals shown in Fig. 3B, the corresponding superimposed spacings are larger by a factor of ~1.4, indicating that these are distinctly different phases.

DISCUSSION

We show in this study that the crystalline structure of microscopic single crystals nucleating in model as well as in native human biles can be determined by cryogenic electron diffraction in their natural state, without drying or chemical fixation. Cholesterol crystals imaged by cryo-TEM are usually relatively large (hundreds of nanometers long) before the contrast between them and the background medium is sufficient to clearly distinguish the crystal and obtain a diffraction pattern. Those large crystals are found positioned flat on the microscopy grid and thus give similar diffraction patterns from the same zone axis. Our data reveal that biliary cholesterol may, apparently, nucleate as three different crystal structures. One is the stable, classic ChM, and the other two are intermediate, metastable crystalline forms of cholesterol.

It is generally accepted that cholesterol gallstones are composed of ChM crystals, held together by a mucin glycoprotein-rich matrix (25). Some studies have, however, suggested the presence of anhydrous cholesterol within stones (8, 26). There have even been claims that anhydrous cholesterol is the principal constituent of cholesterol gallstones (27). Studies on the crystallization process in model biles have revealed a variety of cholesterol crystal forms, some of which have a needle-like morphology, characteristic of anhydrous crystals (10). Those crystals were also found to have a mass density compatible with anhydrous crystals (12, 28). Similar crystal forms were subsequently found also in native human biles (11). Moreover, X-ray powder diffraction data have suggested the presence of anhydrous crystallization during the early stages of crystal formation in model bile (10). Despite all those suggestions, there has been so far no solid proof of the presence or role of anhydrous cholesterol crystallization in the process of gallstone formation. The main reason for this shortcoming was the inability to determine the accurate crystal structure of single crystals within nucleating biles or gallstones. In the present study, we provide the tools for dealing with this question.

Our findings confirm that there is crystallization of ChM in model as well as in native human biles. Because ChM crystals were seen in all crystallizing native biles investigated, as well as in Model A, which simulates lithogenic human gallbladder bile, monohydrate crystallization seems to be the primary crystal form in gallstone patients. Moreover, the fact that ChM crystals were found after prolonged periods of incubation in both models and in the native biles further confirms the notion that monohydrate is the preferred crystalline form in bile at (thermodynamic) equilibrium. Monohydrate crystals were recorded early, as well as late, during the crystallization process, in a variety of crystal morphologies. This underscores that the microscopic crystal habit of cholesterol does not always correlate with the crystal structure, as suggested by experimental data obtained from solvated and nonsolvated crystals (29). The final crystal habit of ChM crystals may relate to the pathway by which they are formed. It is not possible, using cryo-TEM, to follow one crystal throughout its growth, so the exact development of each crystal is still unknown. However, it seems reasonable that stable, micron-sized, plate-like, rhomboidal ChM crystals may originate from early-appearing ChM crystals, whereas stable, needle-like or rectangular ChM crystals may stem from the intermediate pathway observed in this study.

This study also clearly shows that a different crystalline form of cholesterol occurs in bile. Two similar yet distinct diffraction patterns were obtained, with systematic absences appearing in the later, more-stable form. We refer to these phases as the cholesterol intermediate (ChIn) crystalline phases. Solomonov et al. (24) studied cholesterol crystallizing at the air–water interface by grazing-angle X-ray diffraction. In their work, they also observed a metastable form, matching the later-appearing ChIn that led to classic ChM. Given that both studies, using different methodologies and model systems, obtained similar results, the likelihood of these results being artifacts is small.

Solomonov et al. (24) explained that the systematic absences in the late ChIn, compared with the early ChIn, are
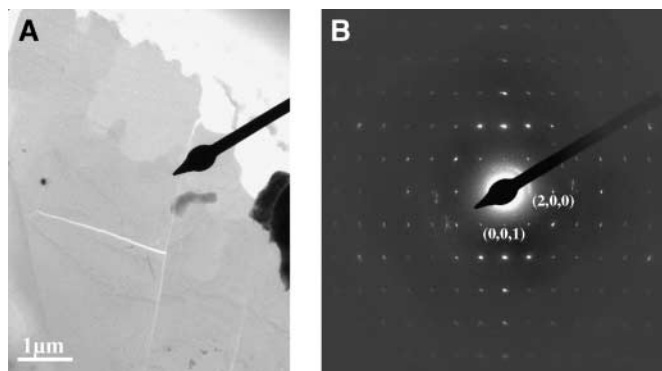

Fig. 4. Standard anhydrous cholesterol crystals. A: Cryo-TEM image. B: Corresponding cryo-ED pattern.

due to the rearrangement of water molecules in the unit cell, leading to increased symmetry of a monoclinic crystal. This diffraction pattern is indexed as a monoclinic ChM phase with reflections {h, k, l = h}, obeying the condition h + l = 2n, having an *mm* symmetry and belonging to the 10 × 7.5 Å unit cell (24). The diffraction pattern of the second ChIn type of crystal was distinct and reproducible. Anhydrous cholesterol had been previously suggested as another form of cholesterol in bile (8, 10). The diffraction pattern from ChIn is distinctly different from the diffraction pattern we obtained from standard anhydrous cholesterol crystals. Solomonov et al. (24) determined the ChIn phase density by least squares from their grazing incidence X-ray diffraction data, measured at 5°C. The calculated density of 1.029(5) gml^{-1} of the multilayer phase was very close to the observed density of 1.032 gml^{-1} of the filamentous crystals detected in model bile by Konikoff et al. (10). Consequently, that may account for the erroneous conclusion (10) that those were anhydrous cholesterol crystals.

The diffraction patterns of the later-appearing ChIn crystals displayed many satellite-like reflections around the main spots (Fig. 3D). These extra spots tended to accentuate the long axis of the crystal, reminiscent of a fiber diffraction pattern. However, in the case of a fiber, the main spots would appear streaked, whereas in our case, the main and satellite spots are round. This could be explained by a multilayered arrangement of the crystal or a liquid crystal structure. Indeed, in the late-appearing ChIn, most of the diffraction patterns were gathered from multilayered crystals (e.g., Fig. 3C). As can be seen in the images, the earliest crystals are small in size but thick enough to be imaged by cryo-TEM with sufficient contrast. Those crystals are either several layers thick or composed of several thinner stacked crystals. Because these crystals seem to be aligned in the same direction, the ensuing diffraction patterns are also aligned, with a relative lateral shift resulting in the satellite points.

The ChIn phase we describe here is identical to the intermediate late appearing ChM phase that had been identified by Leiserowitz and coworkers on the water–air interface (30). In more recent results, the same group (24) has calculated the unit cell parameters of the ChIn. They obtained a monoclinic unit cell with the parameters: a = 10.15 Å, b = 7.57 Å, c = 68.2 Å, α = γ = 90°, and β = 94.8°. The zone axis of the anhydrous cholesterol was [010]. Thus, the a and c lattice parameters of the unit cell can be approximated by d-spacing of the [100] and [001] reflections, respectively. Those parameters were: a = 14.2 Å and c = 10.5 Å. The ratio of those values and the a and b lattice parameters of the transient crystals correspond exactly to the d-spacing factor of 1.4 that we found by superposing the diffraction patterns of the transient and the anhydrous forms.

In the present study, ChIn crystals were detected only in the phospholipid-poor Model B bile. This does not rule out the possibility that this type of transient crystallization occurs in other biles, including native bile. Crystallization via the ChIn route may be of clinical relevance in a select group of patients. Recently, Rosmorduc, Hermelin, and Poupon (31) described a peculiar form of cholesterol gallstone disease in adults. Those patients have a mutation in the phosphatidylcholine translocator gene (MDR3), leading to a phospholipid-poor bile. Similar findings are also seen in experimental animals lacking the translocator (32). The lipid composition of biles from those patients and animals resembles that of Model B in our study, with a high cholesterol-to-phospholipid ratio, and a low phospholipid concentration. The patients have gallbladder as well as intrahepatic cholesterol stones, which is otherwise rare in the Western world. None of our patients had this rare phenotype, and hence ChIn nucleation may have been missed in the present study.

The detailed nucleation pathway leading to ChM in gallstone disease still remains unclear. The tools presented here could provide the means for investigating this question. Further studies combining electron microscopy imaging with targeted electron diffraction may identify ultrastructures and microdomains in which nucleation initiates. Moreover, this approach should also enable time-lapse analysis of crystal transformations during the crystallization process.

In conclusion, we have shown that the combination of cryogenic electron microscopy and electron diffraction allows the detailed study of nucleation of single cholesterol crystals in bile. We have obtained clear, reproducible electron diffraction patterns of cholesterol crystals during the crystallization process in model as well as in human biles. We found that ChM is the principal crystal structure in lithogenic gallbladder bile. However, a different type of monohydrate polymorph nucleates initially in dilute, phospholipid-poor bile. The exact pathophysiological role of this new form of cholesterol crystallization still needs to be determined.🔲🔲

REFERENCES

1. Konikoff, F. M., and J. M. Donovan. 2002. Gallstone disease: pathogenesis and treatment. *In* Schiff's Diseases of the Liver. 9th edition. F. R. Shiff, M. F. Sorrell, and W. C. Maddrey, editors. Lippincott, Williams & Wilkins, Philadelphia. 651–671.
2. Craven, B. M. 1976. Crystal structure of cholesterol monohydrate. *Nature.* **260:** 727–729.
3. Loomis, C. R., G. G. Shipley, and D. M. Small. 1979. The phase behavior of hydrated cholesterol. *J. Lipid Res.* **20:** 525–535.
4. Holan, K. R., R. T. Holzbach, R. E. Hermann, A. M. Cooperman, and W. J. Claffey. 1979. Nucleation time: a key factor in the pathogenesis of cholesterol gallstone disease. *Gastroenterology.* **77:** 611–617.
5. Ogata, T., and Y. Nishie. 1974. A scanning electron microscopic

study on the formation of cholesterol stones. *Tohoku J. Exp. Med.* **113:** 371–381.

6. Abe, A., Y. Tsuchiya, N. Sugiura, H. Saisho, K. Nishimura, and K. Takeo. 1997. Ultrastructure of cholesterol gallstones as observed by electron microscopy after freeze-fracturing. *Tissue Cell.* **29:** 191–197.

7. Bogren, H. 1964. The composition and structure of human gall stones. *Acta Radiol. Diagn. (Stockh).* **13 (Suppl.):** 1–75.

8. Bogren, H., and K. Larsson. 1963. An x-ray-diffraction study of crystalline cholesterol in some pathological deposits in man. *Biochim. Biophys. Acta.* **75:** 65–69.

9. Sutor, D. J., and S. E. Wooley. 1969. X-ray diffraction studies of the composition of gallstones from English and Australian patients. *Gut.* **10:** 681–683.

10. Konikoff, F. M., D. S. Chung, J. M. Donovan, D. M. Small, and M. C. Carey. 1992. Filamentous, helical, and tubular microstructures during cholesterol crystallization from bile. Evidence that biliary cholesterol does not nucleate classic monohydrate plates. *J. Clin. Invest.* **90:** 1155–1160.

11. Wang, D. Q-H., and M. C. Carey. 1996. Characterization of crystallization pathways during cholesterol precipitation from human gallbladder biles: identical pathways to corresponding model biles with three predominating sequences. *J. Lipid Res.* **37:** 2539–2549.

12. Konikoff, F. M., and M. C. Carey. 1994. Cholesterol crystallization from a dilute bile salt-rich model bile. *J. Cryst. Growth.* **144:** 79–86.

13. Kaplun, A., Y. Talmon, F. M. Konikoff, M. Rubin, A. Eitan, M. Tadmor, and D. Lichtenberg. 1994. Direct visualization of lipid aggregates in native human bile by light- and cryo-transmission electron-microscopy. *FEBS Lett.* **340:** 78–82.

14. Kaplun, A., F. M. Konikoff, A. Eitan, M. Rubin, A. Vilan, D. Lichtenberg, T. Gilat, and Y. Talmon. 1997. Imaging supramolecular aggregates in bile models and human bile. *Microsc. Res. Tech.* **39:** 85–96.

15. Konikoff, F. M., D. Danino, D. Weihs, M. Rubin, and Y. Talmon. 2000. Microstructural evolution of lipid aggregates in nucleating model and human biles visualized by cryogenic transmission electron microscopy. *Hepatology.* **31:** 261–268.

16. Konikoff, F. M., H. Laufer, G. Messer, and T. Gilat. 1997. Monitoring cholesterol crystallization from lithogenic model bile by time-lapse density gradient ultracentrifugation. *J. Hepatol.* **26:** 703–710.

17. Carey, M. C. 1978. Critical tables for calculating the cholesterol saturation of native bile. *J. Lipid Res.* **19:** 945–956.

18. Turley, S. D., and J. M. Dietschy. 1978. Re-evaluation of the 3 alpha-hydroxysteroid dehydrogenase assay for total bile acids in bile. *J. Lipid Res.* **19:** 924–928.

19. Siedel, J., E. O. Hagele, J. Ziegenhorn, and A. W. Wahlefeld. 1983. Reagent for the enzymatic determination of serum total cholesterol with improved lipolytic efficiency. *Clin. Chem.* **29:** 1075–1080.

20. Bartlett, G. R. 1959. Phosphorus assay in column chromatography. *J. Biol. Chem.* **234:** 466–468.

21. Bellare, J. R., H. T. Davis, L. E. Scriven, and Y. Talmon. 1988. Controlled environment vitrification system: an improved sample preparation technique. *J. Electron Microsc. Tech.* **10:** 87–111.

22. Talmon, Y. 1983. Staining and drying-induced artifacts in electron microscopy of surfactant dispersions. *J. Colloid Interface Sci.* **93:** 366–381.

23. Gantz, D. L., D. Q-H. Wang, M. C. Carey, and D. M. Small. 1999. Cryoelectron microscopy of a nucleating model bile in vitreous ice: formation of primordial vesicles. *Biophys. J.* **76:** 1436–1451.

24. Solomonov, I., M. J. Weygand, K. Kjaer, H. Rapaport, and L. Leiserowitz. Trapping crystal nucleation of cholesterol monohydrate: relevance to pathological crystallization. *Biophys. J.* In press.

25. Bogren, H. G., H. Mutvei, and G. Renberg. 1995. Scanning electron microscope studies of human gallstones after plasma etching. *Ultrastruct. Pathol.* **19:** 447–453.

26. Amin, A. M., N. Ananthakrishnan, and T. K. Nambinarayanan. 2000. Composition of gallstones and sequential events in biliary lithogenesis—is it different in south India compared to north? *J. Assoc. Physicians India.* **48:** 885–890.

27. Aho, A. J., E. Vilhonen, S. Peltola, and A. Lehtonen. 1985. An x-ray diffraction study of the crystalline composition of gallstones. *Scand. J. Gastroenterol.* **20:** 901–906.

28. Shieh, H. S., L. G. Hoard, and C. E. Nordman. 1977. Crystal structure of anhydrous cholesterol. *Nature.* **267:** 287–289.

29. Garti, N., L. Karpuj, and S. Sarig. 1981. Correlation between crystal habit and the composition of solvated and nonsolvated cholesterol crystals. *J. Lipid Res.* **22:** 785–791.

30. Rapaport, H., I. Kuzmenko, S. Lafont, K. Kjaer, P. B. Howes, J. Als-Nielsen, M. Lahav, and L. Leiserowitz. 2001. Cholesterol monohydrate nucleation in ultrathin films on water. *Biophys. J.* **81:** 2729–2736.

31. Rosmorduc, O., B. Hermelin, and R. Poupon. 2001. MDR3 gene defect in adults with symptomatic intrahepatic and gallbladder cholesterol cholelithiasis. *Gastroenterology.* **120:** 1459–1467.

32. Lammert, F., D. Q-H. Wang, S. Hillebrandt, A. Geier, P. Fickert, M. Trauner, S. Matern, B. Paigen, and M. C. Carey. 2004. Spontaneous cholecysto- and hepatolithiasis in mdr2−/− mice: a model for low phospholipid-associated cholelithiasis. *Hepatology.* **39:** 117–128.